

# Structure–Activity Relationship and Mechanistic Studies of Bisaryl Urea Anticancer Agents Indicate Mitochondrial Uncoupling by a Fatty Acid-Activated Mechanism

Edward York, Daniel A. McNaughton, Ariane Roseblade, Charles G. Cranfield, Philip A. Gale, and Tristan Rawling\*



Cite This: *ACS Chem. Biol.* 2022, 17, 2065–2073



Read Online

ACCESS |



Metrics & More

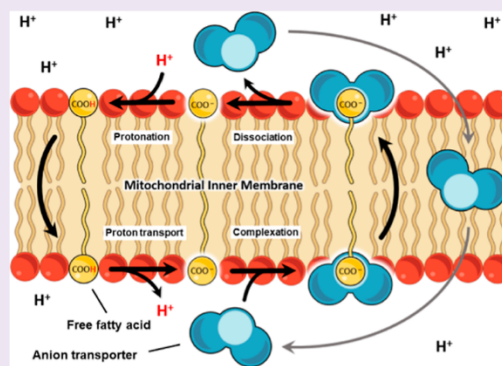


Article Recommendations



Supporting Information

**ABSTRACT:** Targeting the cancer cell mitochondrion is a promising approach for developing novel anticancer agents. The experimental anticancer agent *N,N'*-bis(3,5-dichlorophenyl)urea (SR4) induces apoptotic cell death in several cancer cell lines by uncoupling mitochondrial oxidative phosphorylation (OxPhos) using a protein-free mechanism. However, the precise mechanism by which SR4 depolarizes mitochondria is unclear because SR4 lacks an acidic functional group typically found in protein-independent uncouplers. Recently, it was shown that structurally related thioureas can facilitate proton transport across lipid bilayers by a fatty acid-activated mechanism, in which the fatty acid acts as the site of protonation/deprotonation and the thiourea acts as an anion transporter that shuttles deprotonated fatty acids across the phospholipid bilayer to enable proton leak. In this paper, we show that SR4-mediated proton transport is enhanced by the presence of free fatty acids in the lipid bilayer, indicating that SR4 uncouples mitochondria through the fatty acid-activated mechanism. This mechanistic insight was used to develop a library of substituted bisaryl ureas for structure–activity relationship studies and subsequent cell testing. It was found that lipophilic electron-withdrawing groups on bisaryl ureas enhanced electrogenic proton transport via the fatty acid-activated mechanism and had the capacity to depolarize mitochondria and reduce the viability of MDA-MB-231 breast cancer cells. The most active compound in the series reduced cell viability with greater potency than SR4 and was more effective at inhibiting adenosine triphosphate production.



## INTRODUCTION

The discovery of cytotoxic agents that selectively target cancer cells is critical to the development of well-tolerated anticancer therapeutics. Cancer cell mitochondria have emerged as a promising anticancer drug target because they are structurally and functionally distinct from mitochondria in noncancerous cells and because of their central role in cellular metabolism and apoptosis.<sup>1</sup> Mitochondria are the site of oxidative phosphorylation (OxPhos), a process that converts nutrients into adenosine triphosphate (ATP). OxPhos commences in the mitochondrial matrix, the central region of mitochondria enclosed by the mitochondrial inner membrane (MIM), where nutrients are oxidized to form nicotinamide adenine dinucleotide (NADH) and flavin adenine dinucleotide (FADH<sub>2</sub>). NADH and FADH<sub>2</sub> feed high-energy electrons into the electron transport chain (ETC), a series of proteins embedded in the MIM. As electrons pass through the ETC, protons are pumped from the matrix and into the intermembrane space, generating a proton gradient across the MIM. The resultant mitochondrial membrane potential ( $\Delta\psi_M$ ) drives the flow of protons back into the matrix through the MIM-embedded protein ATP synthase, which catalyzes the

formation of ATP.<sup>2–4</sup> Thus, nutrient oxidation is coupled to ATP formation by the  $\Delta\psi_M$ . In cancer cells, deregulated mitochondrial metabolism results in a shift toward glycolysis and an increased mitochondrial  $\Delta\psi_M$  compared to noncancerous cells.<sup>5</sup> Indeed, hyperpolarization of the MIM is a universal feature of cancer cells, and targeting  $\Delta\psi_M$  may produce novel drugs that selectively target cancer cells.<sup>6–8</sup>

Mitochondrial uncouplers are compounds that uncouple nutrient oxidation from ATP production by collapsing  $\Delta\psi_M$ .<sup>9</sup> The most common uncouplers are protonophores, which are lipophilic weak acids that can shuttle protons across membranes such as the MIM via the protonophoric cycle (Figure 1a). The deprotonated uncoupler ( $A^-$ ) accepts a proton in the intermembrane space and diffuses across the

Received: October 12, 2021

Accepted: July 5, 2022

Published: July 19, 2022



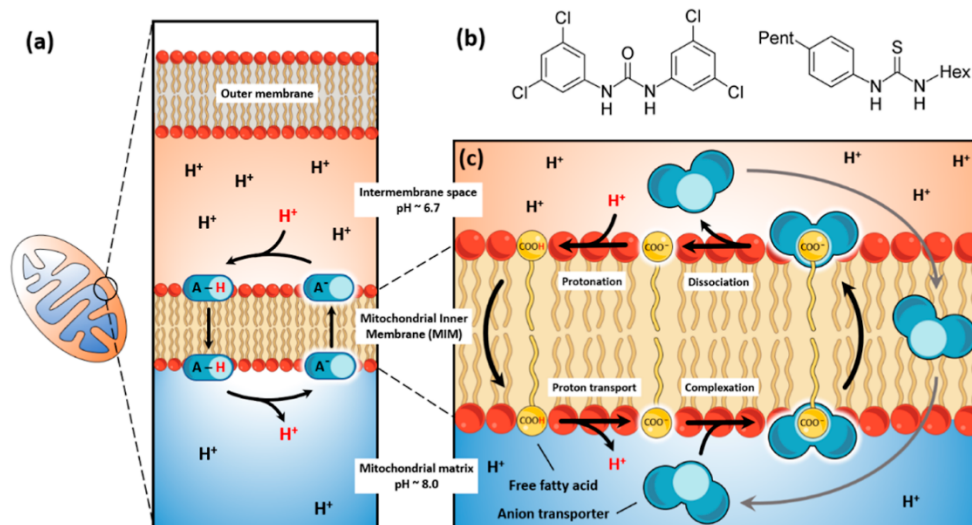


**Figure 1.** Proton transport and mitochondrial uncoupling by protonophoric and fatty acid-activated mechanisms. (a) Mitochondrial uncoupling by classical protonophores. The protonophoric cycle that results in the transport of protons across the MIM and mitochondrial uncoupling. The rate-determining step is diffusion of the anionic species across the MIM. To complete this step, the negative charge is delocalized across an extended  $\pi$ -system to produce a MIM-permeable anion. (b) Chemical structures of SR4 and the structurally related fatty acid-activated thiourea proton transporter, respectively. (c) Fatty acid-activated proton transport mechanism. After deprotonation of the fatty acid in the mitochondrial matrix, the thiourea-based anion transporter binds carboxylate and masks the charge to facilitate fatty acid flip-flop and proton transport across the MIM.

MIM in its neutral form (A–H). Deprotonation of the protonophore in the relatively alkaline matrix results in the transport of one proton across the MIM. For the cycle to continue, the deprotonated protonophore (A<sup>−</sup>) must permeate the MIM and return to the intermembrane space; however, this step is inhibited by the MIM's lipophilic core, which is relatively impermeable to anions.<sup>10,11</sup> Thus, the acidic groups in protonophores are conjugated to extended  $\pi$ -systems, which provide a large surface area for delocalization of the anionic charge. Charge delocalization enhances the lipophilicity and MIM permeability of the anionic protonophore and allows the cycle to continue.<sup>12</sup> Fatty acids such as palmitic acid are weak acids but poor protonophores because insufficient charge delocalization prevents the fatty acid carboxylate from permeating the MIM.<sup>13,14</sup>

The anticancer actions of mitochondrial uncouplers have been increasingly recognized as several uncouplers have been shown to selectively kill cancer cells.<sup>12</sup> One such compound is *N,N'*-bis(3,5-dichlorophenyl)urea (SR4) (Figure 1b), a chlorinated bisaryl urea reported by Figarola et al. to induce apoptotic cell death in leukemia (HL-60), liver (HepG2), and lung (H358) cancer cell lines in vitro.<sup>15–17</sup> SR4 also induces apoptosis in naïve and drug-resistant melanoma (A375 and SK-MEL-28) cell lines<sup>18</sup> and inhibits tumor growth in mouse models of cancer.<sup>17–19</sup> Rigorous mechanistic studies showed that SR4 induces cell death through uncoupling of cancer cell mitochondria and that uncoupling occurs by a protein-independent mechanism. However, the precise mechanism by which SR4-mediated uncoupling occurs has not been determined because SR4 lacks an acidic functional group required for protonophoric activity. Indeed, calculated and experimental  $pK_a$  values of substituted bisaryl ureas range from 14 to 18,<sup>20</sup> which is well above those of previously reported protonophores ( $pK_a$  values range from 4 to 8)<sup>9</sup> and too high to allow protonation/deprotonation at mitochondrial pH.

In 2016, Wu and Gale reported that thiourea-based anion receptors can mediate proton transport across lipid bilayers by

a fatty acid-activated mechanism (Figure 1c), shown using unilamellar vesicles that model the MIM.<sup>21</sup> Similar to the protonophoric cycle, the fatty acid carboxylate is protonated in the intermembrane space and permeates the MIM as a neutral species. Once in the alkaline matrix, the fatty acid is deprotonated, which results in the transport of one proton and the formation of a fatty acid carboxylate that must diffuse back across the MIM. The thiourea next binds to the fatty acid carboxylate group through parallel hydrogen bonds with the thiourea NH groups, which masks the anionic charge to produce a complex that is sufficiently lipophilic to diffuse through the lipid bilayer. Dissociation in the intermembrane space liberates the fatty acid and thiourea, allowing further proton transport to occur. Given that SR4 is structurally similar to the thiourea-based anion receptors and aryl ureas are known anion receptors and transporters,<sup>22–25</sup> and because the MIM contains free fatty acids,<sup>26,27</sup> we suspected that SR4 may uncouple mitochondria by the same fatty acid-activated mechanism. In this paper, we show using an 8-hydroxy-1,3,6-pyrene trisulfonic acid (HPTS) proton transport assay that SR4-mediated proton transport is enhanced by free fatty acids in the bilayer, indicating that SR4 uncouples mitochondria through the fatty acid-activated mechanism. This insight was used to develop a library of substituted bisaryl ureas for structure–activity relationship (SAR) studies and subsequent cell testing. The resulting SAR demonstrated that lipophilic electron-withdrawing groups enhance fatty acid-activated proton transport, and analogues bearing these groups were found to effectively depolarize mitochondria and reduce cell viability in MDA-MB-231 breast cancer cells. The most potent transporter in the series (compound 3) maintained the cellular actions of SR4 and was found to uncouple mitochondrial OxPhos and impair ATP production.

## RESULTS AND DISCUSSION

**SR4-Mediated Proton Transport Is Enhanced in Phospholipid Bilayers Containing Oleic Acid.** To



determine if SR4 can participate in the fatty acid-activated proton transport mechanism identified by Wu and Gale,<sup>21</sup> we used a similar HPTS fluorescence assay to measure electrogenic proton transport in large unilamellar 1-palmitoyl-2-oleoyl-*sn*-glycero-3-phosphocholine (POPC) vesicles (200 nm) in 4-(2-hydroxyethyl)-1-piperazineethanesulfonic acid (HEPES)-buffered potassium gluconate (100 mM) (Figure 2a, see the Supporting Information for details).<sup>28</sup> In this

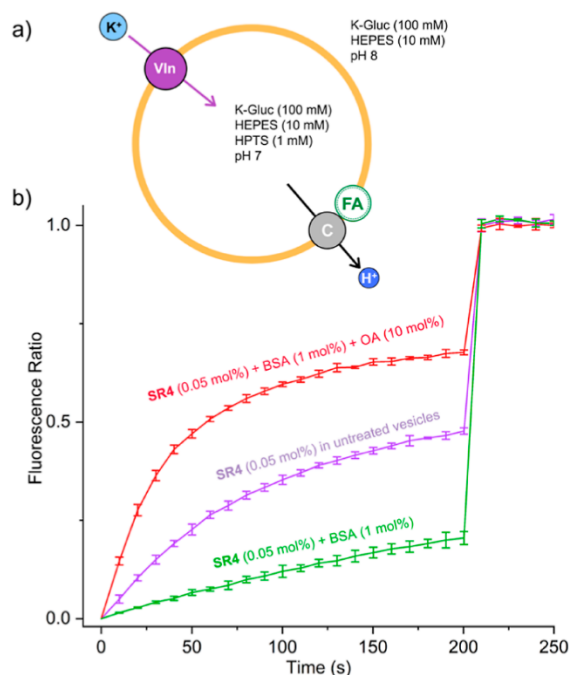


**Figure 2.** (a) Schematic of the HPTS proton transport assay, monitored by HPTS fluorescence, outlining the conditions of the experiment and (b) the proton transport induced by SR4 under the various assay conditions. Vesicles were lysed at 200 s to provide a 100% dissipation reading for calibration purposes. Compound concentrations are represented as compound-to-lipid molar ratios.

system, a pH gradient is established between the interior and exterior environments of the vesicles, and proton transport is measured by monitoring the increase in intravesicular pH using the pH-sensitive fluorescent probe HPTS. SR4-mediated proton transport was tested under three conditions, in untreated POPC vesicles, vesicles pretreated with bovine serum albumin (BSA, 1 mol %), and vesicles pretreated with both BSA (1 mol %) and oleic acid (OA, 10 mol %, corresponding to 4 mol % free concentration after BSA binding). Pretreatment with BSA removes contaminating fatty acids present in POPC to detect proton transport via protonophoric cycling (i.e., classical protonophores). The addition of OA reintroduces the fatty acid-activated mechanism of proton transport, and any enhancement in activity can be assigned to this pathway.

As shown in Figure 2b, SR4-mediated proton transport is diminished in vesicles containing BSA compared to that in untreated vesicles, demonstrating that direct protonophoric cycling cannot explain the observed proton transport facilitated by SR4. This was anticipated because SR4 lacks a functional group sufficiently acidic for deprotonation at mitochondrial pH, and the slight efflux observed may be attributed to the traces of fatty acids that remain in the membrane after BSA treatment.<sup>21</sup> Furthermore, proton transport was enhanced in

the presence of OA, suggesting a fatty acid-dependent pathway. Combined, these data indicate that SR4-mediated proton transport across lipid bilayers is enhanced by free fatty acids and is consistent with the hypothesis that SR4 can act as a fatty acid-activated proton transporter.

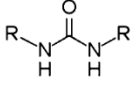
**Compound Library Design and Synthesis.** We next prepared a series of symmetrically substituted bisaryl ureas to determine if the observed SAR was consistent with the fatty acid-activated proton transport mechanism. Under this mechanism, the urea-based anion receptor promotes trans-bilayer movement (“flip-flop”) of anionic fatty acids by binding to and masking the carboxylate charge through parallel hydrogen bonds with the urea N–H groups, producing a complex that is sufficiently lipophilic to permeate lipid bilayers. It was anticipated that electron-withdrawing substituents on the bisaryl urea rings would enhance the carboxylate affinity of the urea binding group, promoting complexation and thus proton transport activity. It was also anticipated that lipophilic substituents would increase complex lipophilicity and improve activity. To test this, a series of symmetrically substituted bisaryl ureas bearing substituents with various electron-withdrawing and -donating capacities (determined from the Hammett substituent constant,  $\sigma$ ) and lipophilic properties (determined from the hydrophobicity constant,  $\pi$ ) were synthesized (Table 1). The compounds were synthesized in one step by the reaction of *N,N'*-carbonyldiimidazole (CDI) with appropriately substituted anilines.

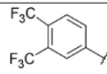
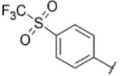
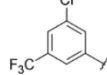
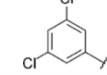
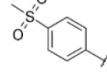
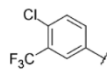
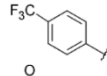
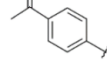
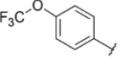
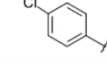
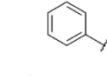
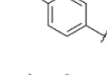
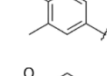
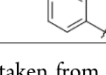
**Bisaryl Ureas Mediate Proton Transport by a Fatty Acid-Activated Mechanism.** We first studied the ability of bisaryl ureas 1–14 to mediate electrogenic proton transport using the HPTS proton transport assay as performed for SR4. Dose–response studies and Hill analyses were performed for compounds 1–14 under three test conditions. An  $EC_{50}$  value, which represents the concentration required to facilitate 50% of the maximum transport, and a Hill coefficient ( $n$ ), which provides an indication of the stoichiometry of the test compound required for the transport process, were calculated for each compound. Initially, the proton transport capability of compounds 1–14 was assessed in untreated vesicles to establish an SAR for the series (Table 1). Subsequently, dose–response studies were performed in the presence of BSA (1 mol %) or in the presence of both BSA (1 mol %) and OA (10 mol %) (Table 2).

Bisaryl ureas 1–SR4 and 6–10 achieved appreciable proton transport below 10 mol % loadings (compound-to-lipid molar ratio) such that  $EC_{50}$  values could be calculated. The remaining compounds at commensurate concentrations did not exhibit significant activity, and higher loadings caused the compounds to precipitate out of aqueous media during experimental runs, meaning  $EC_{50}$  values for the remaining compounds could not be calculated, and compounds were thus considered as inactive.

The SAR elicited from the HPTS assay data of the compounds in untreated vesicles indicates that lipophilic and electron-withdrawing substituents enhance electrogenic proton transport activity. The impact of electron-withdrawing capacity is highlighted clearly as compounds possessing electron-withdrawing substituents all showed appreciable activity apart from urea 5, whereas compounds bearing electron-donating substituents (12, 13, and 14), as well as the unsubstituted urea 11, lacked activity. The importance of lipophilicity can be seen by comparison of ureas 2 and 5. Both compounds share similar electronic and steric properties but differ substantially in

**Table 1.** Chemical Structures, Aromatic Substituent Constants, HPTS (200 s) EC<sub>50</sub> Concentrations, and Hill Coefficients in Untreated POPC Vesicles and MTS (72 h) and JC-1 (1 h) Absolute IC<sub>50</sub> Concentrations Measured in MDA-MB-231 Breast Cancer Cells



Compound	R	$\sigma_{\text{total}}^a$	$\pi_{\text{total}}^a$	HPTS EC <sub>50</sub> (mol%)	Hill (n)	MTS IC <sub>50</sub> ( $\mu\text{M}$ )	JC-1 IC <sub>50</sub> ( $\mu\text{M}$ )
1		1.94	3.52	0.022 ± 0.001	0.91 ± 0.06	0.51 ± 0.1	1.80 ± 0.3
2		1.92	1.10	0.044 ± 0.002	1.38 ± 0.06	0.44 ± 0.1	2.34 ± 0.2
3		1.60	3.18	0.0046 ± 0.0004	0.82 ± 0.07	0.37 ± 0.1	0.26 ± 0.1
SR4		1.48	2.84	0.015 ± 5 × 10 <sup>-4</sup>	1.01 ± 0.04	1.10 ± 0.3	0.45 ± 0.1
5		1.44	-3.26	- <sup>b</sup>	- <sup>b</sup>	- <sup>d</sup>	- <sup>d</sup>
6		1.32	3.18	0.010 ± 9 × 10 <sup>-4</sup>	0.81 ± 0.1	0.68 ± 0.1	1.24 ± 0.3
7		1.08	1.76	0.023 ± 0.001	1.16 ± 0.06	0.84 ± 0.1	2.26 ± 0.4
8		1.00	-1.10	1.61 ± 0.04	1.15 ± 0.05	>100 <sup>c</sup>	22.9 ± 0.4
9		0.70	2.08	0.028 ± 0.005	1.33 ± 0.3	>100 <sup>c</sup>	>100 <sup>c</sup>
10		0.46	1.42	0.11 ± 0.03	2.00 ± 0.6	- <sup>d</sup>	>100 <sup>c</sup>
11		0	0	- <sup>b</sup>	- <sup>b</sup>	>100 <sup>c</sup>	>100 <sup>c</sup>
12		-0.34	1.12	- <sup>b</sup>	- <sup>b</sup>	- <sup>d</sup>	- <sup>d</sup>
13		-0.48	2.24	- <sup>b</sup>	- <sup>b</sup>	- <sup>d</sup>	- <sup>d</sup>
14		-0.54	-0.04	- <sup>b</sup>	- <sup>b</sup>	- <sup>d</sup>	- <sup>d</sup>

<sup>a</sup>Aromatic substituent constants were taken from published values.<sup>29</sup> <sup>b</sup>Did not exceed 50% efflux after 200 s at a loading of 10 mol %. <sup>c</sup>Produced moderate activity at 100  $\mu\text{M}$  but insufficient for absolute IC<sub>50</sub> determination. <sup>d</sup>No activity observed at the maximum test concentration of 100  $\mu\text{M}$ .

lipophilicity. Bisaryl urea **2** is substituted with lipophilic trifluoromethylsulfonyl groups and exhibited an EC<sub>50</sub> of 0.044 mol %. In contrast, while the hydrophilic methanesulfonyl groups of **5** are sufficiently electron-withdrawing, urea **5** lacked activity, presumably because it does not form fatty acid complexes with the lipophilicity required to permeate the lipid bilayer. Polar substituents reduce activity is also supported by urea **8**, which has electron-withdrawing but polar acetyl substituents and was found to be the least potent of the active compounds with an EC<sub>50</sub> of 1.61 mol %.

Compounds with two substituents generally outperformed those with a single para-positioned electron-withdrawing

group. Bisaryl urea **3** was the most potent proton transporter of the series, with an EC<sub>50</sub> value of 0.0046 mol %. **3** closely resembles the structure of **SR4**, bearing a trifluoromethyl group in place of chlorine; however, its 3-fold greater transport activity highlights that modest changes in lipophilic and electronic properties have significant effects on transport activity. However, notably, urea **1** was less effective in the HPTS assays than compounds **3** and **6**, despite the replacement of a second chlorine with another trifluoromethyl substituent. Previous studies by the Gale group and others have highlighted that an optimal degree of lipophilicity is crucial for efficient transport activity.<sup>30,31</sup> Compounds that are

**Table 2.** HPTS EC<sub>50</sub> (200 s) Concentrations and Hill Coefficients in POPC Vesicles in the Presence of BSA and Both BSA and OA

compound	EC <sub>50</sub> (BSA)	<i>n</i> (BSA)	EC <sub>50</sub> (OA)	<i>n</i> (OA)	activation factor <sup>a</sup>
1	0.065 ± 0.003	1.06 ± 0.05	0.014 ± 0.002	0.55 ± 0.1	4.64
2	0.044 ± 0.003	1.26 ± 0.2	0.033 ± 0.001	1.55 ± 0.05	1.33
3	0.06 ± 0.004	1.24 ± 0.09	0.003 ± 1 × 10 <sup>-4</sup>	0.80 ± 0.04	20.00
SR4	0.075 ± 0.009	1.32 ± 0.2	0.00512 ± 4 × 10 <sup>-4</sup>	1.36 ± 0.30	14.65
5	— <sup>b</sup>	— <sup>b</sup>	— <sup>b</sup>	— <sup>b</sup>	— <sup>c</sup>
6	0.098 ± 0.004	1.04 ± 0.1	0.0040 ± 1 × 10 <sup>-4</sup>	1.03 ± 0.03	24.50
7	0.13 ± 0.02	2.00 ± 0.4	0.012 ± 7 × 10 <sup>-4</sup>	1.04 ± 0.03	10.83
8	— <sup>b</sup>	— <sup>b</sup>	0.63 ± 0.07	1.05 ± 0.10	— <sup>c</sup>
9	0.35 ± 0.05	1.56 ± 0.3	0.019 ± 3 × 10 <sup>-4</sup>	1.27 ± 0.03	18.42
10	— <sup>b</sup>	— <sup>b</sup>	0.042 ± 0.004	1.46 ± 0.20	— <sup>c</sup>
11	— <sup>b</sup>	— <sup>b</sup>	— <sup>b</sup>	— <sup>b</sup>	— <sup>c</sup>
12	— <sup>b</sup>	— <sup>b</sup>	— <sup>b</sup>	— <sup>b</sup>	— <sup>c</sup>
13	— <sup>b</sup>	— <sup>b</sup>	— <sup>b</sup>	— <sup>b</sup>	— <sup>c</sup>
14	— <sup>b</sup>	— <sup>b</sup>	— <sup>b</sup>	— <sup>b</sup>	— <sup>c</sup>
CCCP <sup>21</sup>	0.0013	0.97	0.0014	0.99	0.93

<sup>a</sup>EC<sub>50</sub> in the presence of BSA divided by EC<sub>50</sub> in the presence of both BSA and OA. <sup>b</sup>Did not exceed 50% efflux after 200 s at a loading of 10 mol %. <sup>c</sup>The activation factor could not be calculated.

too lipophilic tend to localize in the nonpolar interior of the lipid bilayer and struggle to diffuse into the aqueous phase to complete the transport cycle, resulting in diminished activity.

The EC<sub>50</sub> values determined under the BSA and BSA + OA experimental conditions are shown in Table 2. The enhancement of transport activity in the presence of fatty acid was quantified using an activation factor, calculated by dividing the EC<sub>50</sub> in the presence of BSA by the EC<sub>50</sub> in the presence of both BSA and OA.<sup>21</sup> An activation factor greater than 1 was returned for all compounds with appreciable activity, indicating that dissipation of the proton gradient is enhanced in the presence of fatty acid and, therefore, that the fatty acid-activated mechanism is the dominant pathway of proton transport for the active bisaryl urea compounds.

For comparison, the activation factor previously reported for carbonyl cyanide *m*-chlorophenyl hydrazone (CCCP), a classical protonophore, has been included in Table 2. The activation factor for CCCP is close to one, demonstrating that proton transport facilitated by this compound occurs independently of fatty acids present in the membrane. Notably, urea 2 exhibited only mild activation in the presence of OA and was 10 times less potent than 3, which may be attributed to its markedly lower lipophilicity compared to that of 3. Hill analyses of compounds 8 and 10 for the HPTS assay in the presence of BSA could not be completed due to a lack of transport activity below 10 mol % loading. However, EC<sub>50</sub> values could be determined in the presence of OA and were much lower than the 10 mol % thresholds (0.63 and 0.042 mol %, respectively). This further emphasizes the contribution of the fatty acid-activated mechanism as the main mechanism.

**Mitochondrial Actions of Bisaryl Ureas 1–14.** We next assessed the capacity of bisaryl ureas 1–14 to transport protons across the MIM and depolarize mitochondria in MDA-MB-231 cells using the JC-1 assay. JC-1 is a fluorescent cationic dye that partitions between the mitochondrial matrix and the cytosol according to ΔΨ<sub>M</sub>. In polarized mitochondria with high ΔΨ<sub>M</sub>, JC-1 accumulates in the matrix and forms aggregates that fluoresce red. Upon dissipation of ΔΨ<sub>M</sub> by mitochondrial uncouplers, JC-1 diffuses into the cytosol and disassembles into monomers that fluoresce green. Thus, the JC-1 red/green fluorescence ratio is proportional to the proton

gradient across the MIM. JC-1 IC<sub>50</sub> concentrations for the ureas were determined from dose–response curves as the concentration required to shift the red/green fluorescence ratio by 50% of control (Table 1). One hour treatments were used to distinguish the direct actions of the bisaryl ureas on the MIM from the collapse of ΔΨ<sub>M</sub> that occurs during apoptotic cell death.

The observed JC-1 activity was consistent with the SAR established from the HPTS assay. Analogues that induced mitochondrial depolarization with the lowest JC-1 IC<sub>50</sub> concentrations (1, 2, 3, 6, 7, and SR4) were substituted with lipophilic and electron-withdrawing groups. Polar electron-withdrawing substituents reduced JC-1 activity, as reflected by the inactive urea 5 and urea 8, which had a relatively high IC<sub>50</sub> of 22.9 ± 0.4 μM. The JC-1 results for these analogues follow the HPTS activity trends, and bivariate analysis using log reciprocal transformations of JC-1 IC<sub>50</sub> and HPTS EC<sub>50</sub> concentrations demonstrates a strong positive relationship (*r*<sup>2</sup> = 0.87, Supporting Information, Figure S2). Ureas 9 and 10, which both possess moderately electron-withdrawing substituents (*σ*<sub>total</sub> ≤ 0.70) in para positions, lacked sufficient activity when tested at their solubility limits to calculate JC-1 IC<sub>50</sub> concentrations. These analogues were active in HPTS assays, and the differences may arise from confounding factors (plasma membrane permeability, metabolic stability, etc.) in cell-based assays that are not present in the cell-free HPTS assay. Unsubstituted urea 11 and ureas substituted with electron-donating groups (12, 13, and 14) had poor or no observable activity in both JC-1 and HPTS assays. Taken together, these data support the hypothesis that, like SR4, active bisaryl ureas depolarize mitochondria by the fatty acid-activated mechanism.

Proton transport across the MIM by SR4 leads to mitochondrial uncoupling and reductions in intracellular ATP. To confirm that the most potent urea 3 also produces these actions, we examined each one of these steps.

First, we showed that 3 was a mitochondrial uncoupler using the Seahorse Mito Stress test, which measures the oxygen consumption rate (OCR) of MDA-MB-231 cells. Treatment of the cells with the ATP synthase inhibitor oligomycin reduces the electron flow through the ETC and lowers OCR. Addition



of an uncoupler under these conditions collapses the proton gradient across the MIM and allows unimpeded ETC activity that is observed as an increase in OCR.<sup>32</sup> As shown in Figure 3,

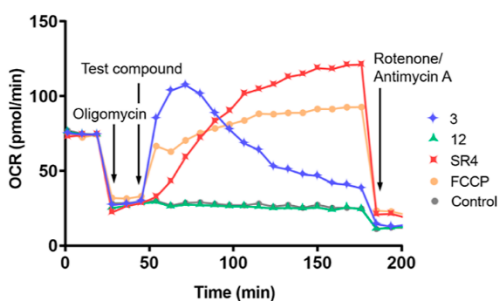


**Figure 3.** OCR in MDA-MB-231 cells treated sequentially with the ATP synthase inhibitor oligomycin (1  $\mu$ M), a test compound (5  $\mu$ M SR4, 5  $\mu$ M 3, or 10  $\mu$ M 12), and the ETC complex inhibitors rotenone/antimycin A (1  $\mu$ M). Test compounds were compared against the classical protonophore FCCP (0.5  $\mu$ M) and a 0.1% DMSO vehicle containing no test compound as control.

addition of 3 (5  $\mu$ M), SR4 (5  $\mu$ M), and the classical uncoupler carbonyl cyanide-*p*-trifluoromethoxyphenylhydrazone (FCCP; 0.5  $\mu$ M) increased OCR in MDA-MB-231 cells treated with oligomycin, indicating that 3, like SR4 and FCCP, is a mitochondrial uncoupler. In contrast, urea 12 (10  $\mu$ M) failed to increase OCR, which was anticipated based on its inactivity in the HPTS and JC-1 assays.

ATP production by OxPhos is dependent on the proton gradient across the MIM, and collapse of  $\Delta\psi_{\text{M}}$  by mitochondrial uncouplers inhibits ATP production. We therefore assessed the effects of SR4 and 3 on intracellular ATP levels in MDA-MB-231 cells. The uncoupler FCCP was included for comparison. Similar to previous observations in liver carcinoma (HepG2) and melanoma (A375 and MeWo) cell lines,<sup>15,18</sup> SR4 and FCCP both reduced intracellular ATP levels to  $\sim$ 85% of dimethylsulfoxide (DMSO)-treated control cells over 8 h (Figure 4). Urea 3 had the largest impact on

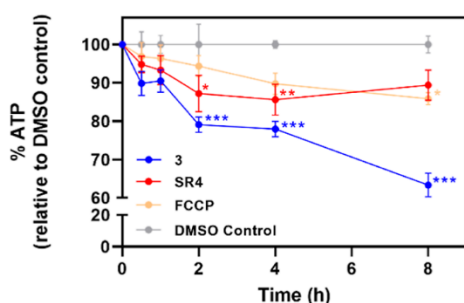


**Figure 4.** Total intracellular ATP levels in MDA-MB-231 cells following treatment with 5  $\mu$ M SR4, 3, FCCP, or vehicle (DMSO) control. ATP levels are expressed as the percentage of the time-matched DMSO control. Different from DMSO-treated control: (\*)  $P < 0.05$ , (\*\*)  $P < 0.01$ , (\*\*\*)  $P < 0.001$ .

intracellular ATP and reduced ATP levels to 60% of the control after 8 h. The higher activity of 3 in this assay is consistent with the higher potencies observed for 3 in the HPTS and JC-1 assays. To confirm that the observed decreases in intracellular ATP were not a result of cell death, LDH release assays were performed. These assays showed that SR4 and 3 did not increase LDH release in MDA-MB-231 cells

compared to control following 8 h treatment (Supporting Information, Figure S6), supporting the conclusion that SR4 and 3 inhibit ATP production. Taken together, these data demonstrate that urea 3 produces similar cellular actions to SR4 in MDA-MB-231 cells by depolarizing mitochondria, uncoupling OxPhos, and inhibiting ATP production.

**Effects of Bisaryl Ureas 1–14 on MDA-MB-231 Cell Viability.** Mitochondrial uncoupling by SR4 is reported to lead to reduction in cancer cell viability,<sup>15,18</sup> so we last assessed the effects of 1–14 on MDA-MB-231 cell viability using MTS assays and compared the findings to the observed SAR from the HPTS and JC-1 data. Dose–response curves (Supporting Information, Figure S3) were constructed from three independent repeats and used to calculate absolute  $\text{IC}_{50}$  concentrations (Table 1). SR4 reduced MDA-MB-231 cell viability with an  $\text{IC}_{50}$  of  $1.1 \pm 0.3 \mu\text{M}$  after 72 h treatment, which is comparable to  $\text{IC}_{50}$  concentrations reported against human HL-60 (1.2  $\mu\text{M}$ , 72 h MTT), HepG2 (3.5  $\mu\text{M}$ , 48 h MTT), and A2058 (5.0  $\mu\text{M}$ , 96 h MTT) cancer cell lines.<sup>15–17</sup> Analogues 1, 2, 3, 6, and 7 reduced MDA-MB-231 cell viability with absolute  $\text{IC}_{50}$  concentrations between 0.3 and 1  $\mu\text{M}$ . Ureas 8 and 9 reduced cell viability at concentrations above 10  $\mu\text{M}$ ; however, absolute  $\text{IC}_{50}$  concentrations could not be calculated for these compounds as they failed to reduce cell viability to below 50% of the control. This activity could indicate that these analogues impact cell viability by affecting progression through the cell cycle, an effect that has been demonstrated for SR4.<sup>15,16</sup> All other bisaryl ureas were essentially inactive, with 11 producing only a moderate reduction in cell viability at the highest test concentration of 100  $\mu\text{M}$ .

Unlike the HPTS data, the MTS  $\text{IC}_{50}$  concentrations calculated for the active compounds were all tightly grouped between 0.37 and 1.10  $\mu\text{M}$ , and the correlation observed between the JC-1 and HPTS results was not found between MTS  $\text{IC}_{50}$  data and HPTS  $\text{EC}_{50}$  data (Supporting Information, Figure S4). One possible explanation is that some of the ureas in the series may be capable of inducing cell death by a second mechanism. For example, pyrimidine-based synthetic anion transporters transport chloride across cellular membranes and have been shown to disrupt intracellular ion homeostasis and induce apoptotic cell death in HeLa and A549 cancer cell lines.<sup>33</sup> Despite this, broad similarities between HPTS and MTS activities remain. All analogues that displayed sufficient activity to calculate absolute MTS  $\text{IC}_{50}$  concentrations (1, 2, 3, 6, 7, and SR4) were substituted with lipophilic electron-withdrawing groups and exhibited proton transport activity in the HPTS assays. Urea 3 was the most active in the series in HPTS, JC-1, and MTS assays and was  $\sim$ 2–3 fold more active than SR4 across all three assays. All analogues that lacked proton transport activity in HPTS assays (5 and 11–14) did not significantly reduce cell viability and were unsubstituted or substituted with polar and/or electron-donating substituents.

Taken together, the data presented in this paper indicate that bisaryl ureas substituted with lipophilic electron-withdrawing groups uncouple mitochondria by the fatty acid-activated mechanism first identified by Wu and Gale<sup>21</sup> and that this uncoupling contributes to the ability of these compounds to reduce cancer cell viability.

## CONCLUSIONS

In this paper, we provide experimental evidence that SR4 uncouples mitochondria by a fatty acid-activated proton

transport mechanism first identified by Wu and Gale. Lipophilic and electron-withdrawing substituents on the bisaryl urea scaffold were shown to enhance electrogenic proton transport using this mechanism, promoting mitochondrial depolarization and reducing cell viability in MDA-MB-231 cells. The SAR is consistent with the proposed fatty acid-activated proton transport mechanism whereby bisaryl ureas facilitate fatty acid flip-flop by binding to fatty acid carboxylate groups to form MIM-permeable complexes. The most potent analogue **3**, like **SR4**, was shown to uncouple mitochondrial OxPhos and inhibit ATP formation in MDA-MB-231 breast cancer cells.

## METHODS

**Chemistry.** CDI, 4-chloro-3-(trifluoromethyl)aniline, and 4-(methylsulfonyl)aniline were purchased from Fluorochem and 3,4-bis(trifluoromethyl)aniline from CombiBlocks. The remaining substituted anilines were purchased from Sigma Aldrich. Reactions were monitored using thin layer chromatography (TLC) on Merck silica gel 60 F<sub>254</sub> aluminum-backed plates. <sup>1</sup>H NMR (500 MHz) and <sup>13</sup>C NMR (125 MHz) spectra were recorded using an Agilent 500 MHz NMR spectrometer. Spectra were referenced internally to the residual solvent (DMSO-*d*<sub>6</sub>: <sup>1</sup>H δ 2.50, <sup>13</sup>C δ 39.52). Melting point determination was performed using a Gallenkamp melting point apparatus. High-resolution mass spectra (HRMS) were recorded on an Agilent Technologies 6510 quadrupole time-of-flight liquid chromatography–mass spectrometer. The purity of all test compounds was confirmed to be >95% by absolute quantitative NMR spectroscopy (Supporting Information, Table S1).

**General Bisaryl Urea Synthesis.** CDI (1.0 mmol) was added to a solution of substituted aniline (2.0 mmol) in anhydrous dichloromethane (DCM, 5 ml) under a nitrogen atmosphere. The solution was refluxed until TLC indicated complete consumption of aniline (6–48 h). The products were purified by one of the following methods:

Method A: The product formed a precipitate in the reaction mixture that was isolated by vacuum filtration and washed with DCM. Any unreacted aniline was then removed by trituration with 1 M HCl (3 × 5 ml).

Method B: The reaction mixture was washed with brine, dried over MgSO<sub>4</sub>, and concentrated under reduced pressure. The resulting solid was trituated with 1 M HCl (3 × 5 ml).

Method C: The reaction mixture was washed with brine, dried over MgSO<sub>4</sub>, and concentrated under reduced pressure. The crude solid was purified by dry column vacuum chromatography using gradient elutions of DCM/EtOAc (100:0 to 85:15).

*N,N'*-Bis[3,4-bis(trifluoromethyl)phenyl]urea (**1**). Purified by method B. Yield: 0.172 g, 32%; mp = 221–222 °C. <sup>1</sup>H NMR (500 MHz, DMSO-*d*<sub>6</sub>): δ 9.76 (s, 2H), 8.22 (s, 2H), 7.95 (d, *J* = 8.5 Hz, 2H), 7.89 (d, *J* = 9). <sup>13</sup>C NMR (125 MHz, DMSO-*d*<sub>6</sub>): δ 152.1 (1C), 143.5 (2C), 129.5 (q, *J* = 6 Hz, 2C), 127.0 (q, *J* = 34 Hz, 2C), 123.1 (q, *J* = 271 Hz, 2C), 122.7 (q, *J* = 272 Hz, 2C), 118.8 (q, *J* = 33 Hz, 2C), 117.2 (q, *J* = 7 Hz, 2C). HRMS (ESI) *m/z*: [M + H]<sup>+</sup> calcd for C<sub>17</sub>H<sub>9</sub>F<sub>12</sub>N<sub>2</sub>O, 485.0518; found, 485.0512.

*N,N'*-Bis[4-(trifluoromethylsulfonyl)phenyl]urea (**2**). Purified by method B. Yield: 0.120 g, 25%; mp = 304–306 °C. <sup>1</sup>H NMR: (500 MHz, DMSO-*d*<sub>6</sub>): δ 9.91 (s, 2H), 8.06 (d, *J* = 9.0 Hz, 4H), 7.90 (dt, *J* = 9.0, 2.5 Hz, 4H). <sup>13</sup>C NMR: (125 MHz, DMSO-*d*<sub>6</sub>): δ 151.7 (1C), 147.7 (2C), 132.5 (4C), 120.8 (2C), 119.6 (q, *J* = 324 Hz, 2C), 118.9 (4C). HRMS (ESI) *m/z*: [M + H]<sup>+</sup> calcd for C<sub>15</sub>H<sub>11</sub>F<sub>6</sub>N<sub>2</sub>O<sub>5</sub>S<sub>2</sub>, 477.0008; found, 477.0002.

*N,N'*-Bis[3-chloro-5-(trifluoromethyl)phenyl]urea (**3**). Purified by method B. Yield: 0.273 g, 56%; mp = 210–211 °C. <sup>1</sup>H NMR: (500 MHz, DMSO-*d*<sub>6</sub>): δ 9.53 (s, 2H), 7.84 (s, 2H), 7.83 (s, 2H), 7.42 (s, 2H). <sup>13</sup>C NMR: (125 MHz, DMSO-*d*<sub>6</sub>): δ 152.2 (1C), 141.6 (2C), 134.2 (2C), 131.1 (q, *J* = 32 Hz, 2C), 123.3 (q, *J* = 271 Hz, 2C), 121.6 (2C), 118.3 (2C), 113.5 (q, *J* = 4 Hz, 2C). HRMS (ESI) *m/z*: [M + H]<sup>+</sup> calcd for C<sub>15</sub>H<sub>9</sub>Cl<sub>2</sub>F<sub>6</sub>N<sub>2</sub>O, 416.9991; found, 416.9985.

*N,N'*-Bis[3,5-dichlorophenyl]urea (**SR4**). Purified by method A. Yield: 0.190 g, 35%. <sup>1</sup>H and <sup>13</sup>C NMR, mp, and HRMS are in agreement with previously reported data.<sup>19,34</sup>

*N,N'*-Bis[4-(methylsulfonyl)phenyl]urea (**5**). Purified by method A. Yield: 0.100 g, 20%, mp = 301–303 °C. <sup>1</sup>H and <sup>13</sup>C NMR and HRMS are in agreement with previously reported data.<sup>35</sup>

*N,N'*-Bis[4-chloro-3-(trifluoromethyl)phenyl]urea (**6**). Purified by method B. Yield: 0.266 g, 41%; mp = 231–232 °C. <sup>1</sup>H and <sup>13</sup>C NMR and HRMS are in agreement with previously reported data.<sup>36</sup>

*N,N'*-Bis[4-(trifluoromethyl)phenyl]urea (**7**). Purified by method C. Yield: 0.211 g, 43%. <sup>1</sup>H and <sup>13</sup>C NMR, mp, and HRMS are in agreement with previously reported data.<sup>37</sup>

*N,N'*-Bis(4-acetylphenyl)urea (**8**). The reaction volume was increased to 20 ml to accommodate for the low solubility of the 8 carbamoylimidazole intermediate. Purified by method A. Yield: 0.162 g, 33%. <sup>1</sup>H and <sup>13</sup>C NMR, mp, and HRMS are in agreement with previously reported data.<sup>38</sup>

*N,N'*-Bis[4-(trifluoromethoxy)phenyl]urea (**9**). Purified by method A. Yield: 0.191 g, 36%. <sup>1</sup>H and <sup>13</sup>C NMR, mp, and HRMS are in agreement with previously reported data.<sup>39</sup>

*N,N'*-Bis[4-chlorophenyl]urea (**10**). Purified by method A. Yield: 0.383 g, 70%. <sup>1</sup>H and <sup>13</sup>C NMR, mp, and HRMS are in agreement with previously reported data.<sup>40</sup>

*N,N'*-Diphenylurea (**11**). Purified by method A. Yield: 0.340 g, 60%. <sup>1</sup>H and <sup>13</sup>C NMR, mp, and HRMS are in agreement with previously reported data.<sup>37</sup>

*N,N'*-Bis(3,4-dimethylphenyl)urea (**12**). Purified by method A. Yield: 0.363 g, 65%; <sup>1</sup>H and <sup>13</sup>C NMR, mp, and HRMS are in agreement with previously reported data.<sup>40</sup>

*N,N'*-Bis(3,4-dimethylphenyl)urea (**13**). Purified by method A. Yield: 0.212 g, 42%; <sup>1</sup>H and <sup>13</sup>C NMR, mp, and HRMS are in agreement with previously reported data.<sup>41</sup>

*N,N'*-Bis(4-methoxyphenyl)urea (**14**). Purified by method A. Yield: 0.265 g, 48%. <sup>1</sup>H and <sup>13</sup>C NMR, mp, and HRMS are in agreement with previously reported data.<sup>40</sup>

**Cell-Based Assays.** *General.* Human MDA-MB-231 breast cancer cells were obtained from ATCC. Cells were cultured in Dulbecco's modified Eagle's medium containing 10% (v/v) fetal bovine serum (Thermo Fischer Scientific) and 1% (v/v) penicillin/streptomycin (Sigma-Aldrich) at 37 °C in a humidified atmosphere of 5% CO<sub>2</sub>. Confluent cells (80–90%) were harvested with trypsin/ethylenediaminetetraacetic acid (EDTA) after washing in Dulbecco's phosphate-buffered saline (dPBS, Sigma-Aldrich). Cells were treated with various concentrations of the test compounds in DMSO (final concentration 0.1% v/v); control cells were treated with DMSO alone.

*JC-1.* MDA-MB-231 cells were seeded in triplicate in black-wall 96-well plates (1.5 × 10<sup>4</sup> cells per well) in complete media for 24 h before treatment. Media were removed, and cells were treated with various drug concentrations in complete media and incubated for 1 h. Cells were incubated with JC-1 in media for 20 min, washed with dPBS, and read using a Tecan Infinite M1000 Pro plate reader to evaluate red (535 nm) and green (595 nm) fluorescence using excitation wavelengths of 485 and 535 nm, respectively (JC-1 Mitochondrial Membrane Potential Assay kit, Cayman Chemical).

*Seahorse XF Mito Stress Tests.* The mitochondrial function was measured by determining the OCR of cells with a Seahorse XF24 extracellular flux analyzer (Seahorse Bioscience) according to the manufacturer's protocol. MDA-MB-231 cells were seeded in Seahorse XF24 well cell culture microplates (2.0 × 10<sup>4</sup> cells per well) in complete media, allowed to adhere for 3 h at room temperature, and incubated overnight. Well media were replaced with 500 μL of XF media (1 mM pyruvate, 2 mM glutamine, and 10 mM glucose Seahorse XF DMEM, pH 7.4 with 5 mM HEPES) and placed in a non-CO<sub>2</sub> incubator (37 °C, humidified) for 1 h, and then, the OCR was measured utilizing an XF Cell Mito Stress Test kit (Seahorse Bioscience, MA, USA). Oligomycin (final concentration: 1 μM), FCCP (final concentration: 0.5 μM) or test compounds (final concentration: 5 μM or 10 μM), and rotenone/antimycin A (final concentrations: 0.5 μM each) were added to the sensor cartridge, and



the OCR was measured using a modified cycling program on Agilent Seahorse Wave Desktop software.

**Intracellular ATP.** MDA-MB-231 cells were seeded in triplicate in 96-well plates ( $1.0 \times 10^4$  cells per well) in complete media for 24 h before treatment. At different timepoints, media were removed, and cells were treated with test compounds ( $5 \mu\text{M}$ ) and incubated for the duration of the experiment. Cells were incubated with CellTiter-Glo 2.0 in complete media, mixed on an orbital shaker for 2 min, and left at room temperature under dark conditions for 10 min, and luminescence was read on a Tecan Infinite M1000 Pro plate reader (CellTiter-Glo 2.0 Luminescent Cell Viability Assay).

**LDH Release.** MDA-MB-231 cells were seeded in triplicate in 96-well plates ( $1.0 \times 10^4$  cells per well) in complete media for 24 h before treatment. Media were removed, and cells were treated with the test compounds ( $5 \mu\text{M}$ ) or vehicle control and incubated for 8 h. Well media were homogenized gently, sampled, and diluted in LDH storage buffer and stored at  $-20^\circ\text{C}$ , including wells containing the vehicle control treated with 0.2% (v/v) Triton X-100 (Sigma-Aldrich) and incubated for 15 min prior to sampling to obtain a maximum LDH release value. Samples were thawed and incubated with LDH detection reagent in a black-wall plate at room temperature for 1 h, and luminescence was measured on a Tecan infinite M1000 Pro plate reader (LDH-Glo Cytotoxicity Assay, Promega).

**MTS.** MDA-MB-231 cells were seeded in triplicate in 96-well plates ( $3.5 \times 10^3$  cells per well) in complete media and incubated for 24 h before treatment. Media were removed, and cells were treated with various drug concentrations in complete media and incubated for 72 h. Cells were then incubated with the CellTiter MTS 96 Aqueous MTS Reagent Powder (Promega) and phenazine ethosulfate (Sigma-Aldrich) under dark conditions for approximately 3 h. The absorbance of each well at 490 nm was measured using a Tecan Infinite M1000 Pro plate reader to evaluate cell viability (CellTiter 96 Aqueous Non-Radioactive Cell Proliferation Assay, Promega).

**Statistical Analysis.** All data are expressed throughout as means  $\pm$  SEM from three independent experiments ( $N = 3$ ). Dose–response curves were constructed using  $\log(\text{inhibitor})$  versus response, variable slope (four parameters) nonlinear regressions on GraphPad Prism 8. Equation:  $Y = \text{Bottom} + (\text{Top} - \text{Bottom}) / (1 + 10^{[(\text{Log IC}_{50} - X) * \text{HillSlope}]})$ . Absolute  $\text{IC}_{50}$  concentrations were interpolated from these normalized curves (data normalized to the DMSO vehicle control) with the top constrained to 100%. ATP and apoptosis data are expressed as mean percentages of the time-matched DMSO control. (\*)  $P < 0.05$ , (\*\*)  $P < 0.01$ , (\*\*\*)  $P < 0.001$  versus time-matched control by two-way analysis of variance with Dunnett's multiple comparison test. Seahorse data were normalized to the baseline OCR prior to oligomycin addition.

## ■ ASSOCIATED CONTENT

### SI Supporting Information

The Supporting Information is available free of charge at <https://pubs.acs.org/doi/10.1021/acscchembio.1c00807>.

HPTS proton transport assay protocol, bisaryl urea absolute quantitative  $^1\text{H}$  NMR purity determination, representative JC-1/MTS dose–response curves, ATP assay data distribution, LDH release cytotoxicity assay, bisaryl urea  $^1\text{H}$  and  $^{13}\text{C}$  NMR spectra, and HPTS dose–response and Hill analyses (PDF)

## ■ AUTHOR INFORMATION

### Corresponding Author

Tristan Rawling – School of Mathematical and Physical Sciences, Faculty of Science, University of Technology Sydney, Sydney, NSW 2007, Australia; [orcid.org/0000-0002-6624-6586](https://orcid.org/0000-0002-6624-6586); Email: [Tristan.Rawling@uts.edu.au](mailto:Tristan.Rawling@uts.edu.au)

## Authors

Edward York – School of Mathematical and Physical Sciences, Faculty of Science, University of Technology Sydney, Sydney, NSW 2007, Australia

Daniel A. McNaughton – School of Chemistry, The University of Sydney, Sydney, NSW 2006, Australia

Ariane Roseblade – School of Mathematical and Physical Sciences, Faculty of Science, University of Technology Sydney, Sydney, NSW 2007, Australia

Charles G. Cranfield – School of Life Sciences, Faculty of Science, University of Technology Sydney, Sydney, NSW 2007, Australia; [orcid.org/0000-0003-3608-5440](https://orcid.org/0000-0003-3608-5440)

Philip A. Gale – School of Chemistry and The University of Sydney Nano Institute (SydneyNano), The University of Sydney, Sydney, NSW 2006, Australia

Complete contact information is available at:

<https://pubs.acs.org/10.1021/acscchembio.1c00807>

## Notes

The authors declare no competing financial interest.

## ■ ACKNOWLEDGMENTS

The author acknowledges H. Macdermott-Opeskin for his assistance in preparing the manuscript. D.A.M. and P.A.G. acknowledge and pay respect to the Gadigal people of the Eora Nation, the traditional owners of the land on which we research, teach, and collaborate at the University of Sydney. P.A.G. thanks the University of Sydney and the Australian Research Council (DP200100453) for funding.

## ■ REFERENCES

- (1) Fulda, S.; Galluzzi, L.; Kroemer, G. Targeting mitochondria for cancer therapy. *Nat. Rev. Drug Discovery* **2010**, *9*, 447–464.
- (2) Cooper, G. M. The Mechanism of Oxidative Phosphorylation *The Cell: A Molecular Approach*, 2nd ed, 2000.
- (3) Lodish, H.; Berk, A.; Zipursky, S. L.; Matsudaira, P.; Baltimore, D.; Darnell, J. Electron Transport and Oxidative Phosphorylation, *Molecular Cell Biology*, 4th ed, 2000.
- (4) Papa, S.; Martino, P. L.; Capitanio, G.; Gaballo, A.; De Rasmio, D.; Signorile, A.; Petruzzella, V. The oxidative phosphorylation system in mammalian mitochondria. *Adv. Exp. Med. Biol.* **2012**, *942*, 3–37.
- (5) Weinberg, S. E.; Chandel, N. S. Targeting mitochondria metabolism for cancer therapy. *Nat. Chem. Biol.* **2015**, *11*, 9–15.
- (6) Gogvadze, V.; Orrenius, S.; Zhivotovsky, B. Mitochondria in cancer cells: what is so special about them? *Trends Cell Biol* **2008**, *18*, 165–173.
- (7) Bonnet, S.; Archer, S. L.; Allalunis-Turner, J.; Haromy, A.; Beaulieu, C.; Thompson, R.; Lee, C. T.; Lopaschuk, G. D.; Puttagunta, L.; Bonnet, S.; et al. A Mitochondria-K<sup>+</sup> Channel Axis Is Suppressed in Cancer and Its Normalization Promotes Apoptosis and Inhibits Cancer Growth. *Cancer Cell* **2007**, *11*, 37–51.
- (8) Heerdt, B. G.; Houston, M. A.; Augenlicht, L. H. The intrinsic mitochondrial membrane potential of colonic carcinoma cells is linked to the probability of tumor progression. *Cancer Res.* **2005**, *65*, 9861–9867.
- (9) Childress, E. S.; Alexopoulos, S. J.; Hoehn, K. L.; Santos, W. L. Small Molecule Mitochondrial Uncouplers and Their Therapeutic Potential. *J. Med. Chem.* **2018**, *61*, 4641–4655.
- (10) Ripoll, C.; Roldan, M.; Contreras-Montoya, R.; Diaz-Mochon, J. J.; Martin, M.; Ruedas-Rama, M. J.; Orte, A. Mitochondrial pH Nanosensors for Metabolic Profiling of Breast Cancer Cell Lines. *Int. J. Mol. Sci.* **2020**, *21*, 3731.
- (11) Benz, R.; McLaughlin, S. The molecular mechanism of action of the proton ionophore FCCP (carbonyl cyanide p-trifluoromethoxyphenylhydrazone). *Biophys. J.* **1983**, *41*, 381–398.



- (12) Shrestha, R.; Johnson, E.; Byrne, F. L. Exploring the therapeutic potential of mitochondrial uncouplers in cancer. *Mol. Metab.* **2021**, *51*, 101222.
- (13) Di Paola, M.; Lorusso, M. Interaction of free fatty acids with mitochondria: coupling, uncoupling and permeability transition. *Biochim. Biophys. Acta* **2006**, *1757*, 1330–1337.
- (14) Wojtczak, L.; Wię, M. R.; Schönfeld, P. Protonophoric activity of fatty acid analogs and derivatives in the inner mitochondrial membrane: a further argument for the fatty acid cycling model. *Arch. Biochem. Biophys.* **1998**, *357*, 76–84.
- (15) Figarola, J. L.; Singhal, J.; Tompkins, J. D.; Rogers, G. W.; Warden, C.; Horne, D.; Riggs, A. D.; Awasthi, S.; Singhal, S. S. SR4 Uncouples Mitochondrial Oxidative Phosphorylation, Modulates AMP-dependent Kinase (AMPK)-Mammalian Target of Rapamycin (mTOR) Signaling, and Inhibits Proliferation of HepG2 Hepatocarcinoma Cells. *J. Biol. Chem.* **2015**, *290*, 30321–30341.
- (16) Figarola, J. L.; Weng, Y.; Lincoln, C.; Horne, D.; Rahbar, S. dichlorophenyl urea compounds inhibit proliferation of human leukemia HL-60 cells by inducing cell cycle arrest, differentiation and apoptosis. *Invest. New Drugs* **2012**, *30*, 1413–1425.
- (17) Singhal, S. S.; Figarola, J.; Singhal, J.; Leake, K.; Nagaprashantha, L.; Lincoln, C.; Gabriel Gugiu, G. B.; Horne, D.; Jove, R.; Awasthi, S.; et al. 1,3-Bis(3,5-dichlorophenyl) urea compound 'COH-SR4' inhibits proliferation and activates apoptosis in melanoma. *Biochem. Pharmacol.* **2012**, *84*, 1419–1427.
- (18) Figarola, J. L.; Singhal, J.; Singhal, S.; Kusari, J.; Riggs, A. Bioenergetic modulation with the mitochondria uncouplers SR4 and Niclosamide prevents proliferation and growth of treatment-I and vemurafenib-resistant melanomas. *Oncotarget* **2018**, *9*, 36945–36965.
- (19) Singhal, S. S.; Figarola, J.; Singhal, J.; Nagaprashantha, L.; Berz, D.; Rahbar, S.; Awasthi, S. Novel compound 1,3-bis (3,5-dichlorophenyl) urea inhibits lung cancer progression. *Biochem. Pharmacol.* **2013**, *86*, 1664–1672.
- (20) Ho, J.; Zwicker, V. E.; Yuen, K. K. Y.; Jolliffe, K. A. Quantum Chemical Prediction of Equilibrium Acidities of Ureas, Deltamides, Squaramides, and Croconamides. *J. Org. Chem.* **2017**, *82*, 10732–10736.
- (21) Wu, X.; Gale, P. A. Small-Molecule Uncoupling Protein Mimics: Synthetic Anion Receptors as Fatty Acid-Activated Proton Transporters. *J. Am. Chem. Soc.* **2016**, *138*, 16508–16514.
- (22) Gale, P. A.; Davis, J. T.; Quesada, R. Anion transport and supramolecular medicinal chemistry. *Chem. Soc. Rev.* **2017**, *46*, 2497–2519.
- (23) Davis, J. T.; Gale, P. A.; Quesada, R. Advances in anion transport and supramolecular medicinal chemistry. *Chem. Soc. Rev.* **2020**, *49*, 6056–6086.
- (24) Blažek Bregović, V.; Basarić, N.; Mlinarić-Majerski, K. Anion binding with urea and thiourea derivatives. *Coord. Chem. Rev.* **2015**, *295*, 80–124.
- (25) Amendola, V.; Fabbri, L.; Mosca, L. Anion recognition by hydrogen bonding: urea-based receptors. *Chem. Soc. Rev.* **2010**, *39*, 3889–3915.
- (26) Penzo, D.; Tagliapietra, C.; Colonna, R.; Petronilli, V.; Bernardi, P. Effects of fatty acids on mitochondria: implications for cell death. *Biochim. Biophys. Acta. Bioenerg.* **2002**, *1555*, 160–165.
- (27) Antonenko, Y. N.; Avetisyan, A. V.; Cherepanov, D. A.; Knorre, D. A.; Korshunova, G. A.; Markova, O. V.; Ojovan, S. M.; Perevoshchikova, I. V.; Pustovidko, A. V.; Rokitskaya, T. I.; et al. Derivatives of rhodamine 19 as mild mitochondria-targeted cationic uncouplers. *J. Biol. Chem.* **2011**, *286*, 17831–17840.
- (28) Gilchrist, A. M.; Wang, P.; Carreira-Barral, I.; Alonso-Carrillo, D.; Wu, X.; Quesada, R.; Gale, P. A. Supramolecular methods: the 8-hydroxypyrene-1,3,6-trisulfonic acid (HPTS) transport assay. *Supramol. Chem.* **2021**, *1*–20.
- (29) Hansch, C.; Leo, A.; Unger, S. H.; Kim, K. H.; Nikaitani, D.; Lien, E. J. Aromatic substituent constants for structure-activity correlations. *J. Med. Chem.* **1973**, *16*, 1207–1216.
- (30) Saggiomo, V.; Otto, S.; Marques, I.; Félix, V.; Torroba, T.; Quesada, R. The role of lipophilicity in transmembrane anion transport. *ChemComm* **2012**, *48*, 5274–5276.
- (31) Knight, N. J.; Hernando, E.; Haynes, C. J. E.; Busschaert, N.; Clarke, H. J.; Takimoto, K.; García-Valverde, M.; Frey, J. G.; Quesada, R.; Gale, P. A. QSAR analysis of substituent effects on tambjamine anion transporters. *Chem. Sci.* **2016**, *7*, 1600–1608.
- (32) Plitzko, B.; Loesgen, S. Measurement of Oxygen Consumption Rate (OCR) and Extracellular Acidification Rate (ECAR) in Culture Cells for Assessment of the Energy Metabolism. *Bio. Protoc.* **2018**, *8*, No. e2850.
- (33) Ko, S.-K.; Kim, S. K.; Share, A.; Lynch, V. M.; Park, J.; Namkung, W.; Van Rossom, W.; Busschaert, N.; Gale, P. A.; Sessler, J. L.; et al. Synthetic ion transporters can induce apoptosis by facilitating chloride anion transport into cells. *Nat. Chem.* **2014**, *6*, 885–892.
- (34) Ricci, A.; Carra, A.; Rolli, E.; Bertoletti, C.; Morini, G.; Incerti, M.; Vicini, P. Effect of Cl-Substitution on Rooting- or Cytokinin-like Activity of Diphenylurea Derivatives. *J. Plant Growth Reg.* **2004**, *23*, 261–268.
- (35) Marshall, S. R.; Singh, A.; Wagner, J. N.; Busschaert, N. Enhancing the selectivity of optical sensors using synthetic transmembrane ion transporters. *ChemComm* **2020**, *56*, 14455–14458.
- (36) Denoyelle, S.; Chen, T.; Chen, L.; Wang, Y.; Klosi, E.; Halperin, J. A.; Aktas, B. H.; Chorev, M. In vitro inhibition of translation initiation by N,N'-diarylureas—potential anti-cancer agents. *Bioorg. Med. Chem. Lett.* **2012**, *22*, 402–409.
- (37) Busschaert, N.; Kirby, I. L.; Young, S.; Coles, S. J.; Horton, P. N.; Light, M. E.; Gale, P. A. Squaramides as potent transmembrane anion transporters. *Angew. Chem., Int. Ed. Engl.* **2012**, *51*, 4426–4430.
- (38) Guan, Z.-H.; Lei, H.; Chen, M.; Ren, Z.-H.; Bai, Y.; Wang, Y.-Y. Palladium-Catalyzed Carbonylation of Amines: Switchable Approaches to Carbamates and N,N'-Disubstituted Ureas. *Adv. Synth. Catal.* **2012**, *354*, 489–496.
- (39) Wang, M.; Han, J.; Si, X.; Hu, Y.; Zhu, J.; Sun, X. Effective approach to ureas through organocatalyzed one-pot process. *Tetrahedron Lett.* **2018**, *59*, 1614–1618.
- (40) Pfeifer, L.; Engle, K. M.; Pidgeon, G. W.; Sparkes, H. A.; Thompson, A. L.; Brown, J. M.; Gouverneur, V. Hydrogen-Bonded Homoleptic Fluoride-Diarylurea Complexes: Structure, Reactivity, and Coordinating Power. *J. Am. Chem. Soc.* **2016**, *138*, 13314–13325.
- (41) Zhou, S.; Yao, T.; Yi, J.; Li, D.; Xiong, J. A Simple and Efficient Synthesis of Diaryl Ureas with Reduction of the Intermediate Isocyanate by Triethylamine. *J. of Chem. Res.* **2013**, *37*, 315–319.

